Analytical Solutions for Spontaneous Imbibition: Fractional-Flow Theory and Experimental Analysis

K. S. Schmid, The Boston Consulting Group; **N. Alyafei,** Texas A&M University at Qatar; **S. Geiger,** Heriot-Watt University; and **M. J. Blunt,** Imperial College London

Summary

We present analytical solutions for capillary-controlled displacement in one dimension by use of fractional-flow theory. We show how to construct solutions with a spreadsheet that can be used for the analysis of experiments as well as matrix-block-scale recovery in field settings. The solutions can be understood as the capillary analog to the classical Buckley-Leverett solution (Buckley and Leverett 1942) for viscous-dominated flow, and are valid for cocurrent and countercurrent spontaneous imbibition (SI), as well as for arbitrary capillary pressure and relative permeability curves. They can be used to study the influence of wettability, predicting saturation profiles and production rates characteristic for water-wet and mixed-wet conditions. We compare our results with in-situ measurements of saturation profiles for SI in a water-wet medium. We show that the characteristic shape of the saturation profile is consistent with the expected form of the relative permeabilities. We discuss how measurements of imbibition profiles, in combination with other measurements, could be used to determine relative permeability and capillary pressure.

Introduction

SI has received considerable attention in the literature because it is one of the key production mechanisms in fractured reservoirs that host the majority of the world's remaining conventional oil. SI can occur in countercurrent and cocurrent mode. In countercurrent imbibition, water and oil both flow through the inlet of a core or matrix block but in opposite directions, whereas in cocurrent imbibition, oil and water flow in the same direction and the oil leaves through the other end. Both cocurrent and countercurrent SI are important in fractured reservoirs. If the matrix blocks are not fully surrounded by water, countercurrent imbibition prevails. Otherwise, cocurrent imbibition is dominant (Bourbiaux and Kalaydjian 1990; Pooladi-Darvish and Firoozabadi 2000). The difference between these mechanisms is crucial because experiments and numerical studies alike show that recovery rates and displacement efficiency are significantly higher in the case of cocurrent imbibition (Bourbiaux and Kalaydjian 1990; Pooladi-Darvish and Firoozabadi 2000; Chen et al. 2003). Therefore, any complete analytical description of SI must not only be capable of accounting for all relevant petrophysical properties, such as wetting and fluid properties, but must also be able to distinguish between cocurrent and countercurrent SI.

Although an analytical solution for purely advective flow has been known for decades—the classical Buckley-Leverett solution (Buckley and Leverett 1942)—its analytical counterpart for capillary-driven flow (SI) is less well-established in the literature (Schmid et al. 2011; Schmid and Geiger 2012, 2013). Given the outstanding practical importance of SI and the usefulness of analytical solutions, many authors have tried to obtain solutions for this situation. However, because the underlying strong nonlinearities pose significant mathematical difficulties, most analytical solutions made additional assumptions, such as specific relative permeability curves (Yortsos and Fokas 1983), a linear capillary pressure–saturation relationship (Cil and Reis 1996), or steady-state flow (Kashchiev and Firoozabadi 2002). Barenblatt et al. (1990) provides a review of the traditional mathematical treatment of SI.

McWhorter and Sunada (1990) reported analytical solutions for cocurrent and countercurrent imbibition where no such additional assumptions were made. However, their mathematical formalism required that the boundary conditions for the water inflow be stated in a specific way, which led all subsequent authors—including McWhorter and Sunada (1992) themselves—to believe that the solution obtained was yet another specific case, and the search for a general solution continued (Kashchiev and Firoozabadi 2002). Schmid et al. (2011) recently proved that the situation described by McWhorter and Sunada (1990) is a general, closed-form solution for SI, and showed that formally the solution might be understood as the Buckley-Leverett analog of SI. Later Schmid and Geiger (2012) showed that on the basis of this closed-form solution, the general nondimensional time or "scaling group" for SI can be obtained. Contrary to all other scaling equations, their scaling group does not require fitting parameters, and independent of rock and fluid type reliably scales water-wet (Schmid and Geiger 2012) and mixed-wet (Schmid and Geiger 2013) experiments. The closed-form solutions for SI, however, can look mathematically challenging because they require the calculation of two implicit integrals. This mathematical difficulty can easily obscure the simple physical meaning of the solution and make its presentation appear much more difficult than the Buckley-Leverett solution (Mason and Morrow 2013). The aim of this paper is therefore to give a novel introduction to the analytical solution for SI by use of physical reasoning, simplifying the mathematical formalism presented previously (McWhorter and Sunada 1990; Schmid et al. 2011) in a way that makes it accessible to anyone with some understanding of the Buckley-Leverett method and fractional-flow theory. We also provide a novel but simple way of calculating the solution in a spreadsheet[1]. We then compare with measured saturation profiles for cocurrent SI and show how the analytical solutions can be used to constrain relative permeability and capillary pressure, as a complement to other types of measurement.

The paper is structured as follows. We start with introducing the equations for linear, incompressible two-phase flow. We show how, on physical grounds, an analytical solution for cocurrent and countercurrent SI can be derived in a way similar to the Buckley-Leverett theory, and how it can easily be computed with a simple spreadsheet. In the example section, we illustrate how to obtain the solution for water-wet and mixed-wet rocks. The examples also demonstrate how the analytical solutions predict the difference between cocurrent and countercurrent SI, and the influence of wetting behavior on displacement efficiency and recovery rates. In the application section, we compare our solutions with measured saturation profiles and use the theory to constrain the relative permeabilities and capillary pressures. The use of SI solutions to match to saturation measurements during SI, combined with other measurements to determine relative permeability and capillary pressure, is discussed.

Original SPE manuscript received for review 4 August 2014. Revised manuscript received for review 18 May 2016. Paper (SPE 184393) peer approved 17 August 2016.

[1] The spreadsheets can be downloaded from https://www.imperial.ac.uk/engineering/departments/earth-science/research/research-groups/perm/research/pore-scale-modelling/software/ and http://carbonates.hw.ac.uk/software.html.

Two-Phase-Flow Equations

We consider 1D flow of two immiscible, incompressible phases through a homogeneous porous medium. Conservation of mass (strictly, volume) can be written as

$$\phi \frac{\partial S_w}{\partial t} + \frac{\partial q_w}{\partial x} = 0, \quad \ldots\ldots\ldots\ldots\ldots\ldots\ldots\ldots (1)$$

where ϕ is the porosity; S_w and S_o are the water and oil saturation, respectively; and q_w is the water velocity (Dake 1983; Helmig 1997):

$$q_w = \frac{\lambda_w}{\lambda_t} q_t + K \frac{\lambda_w \lambda_o}{\lambda_t} \frac{\mathrm{d}p_c}{\mathrm{d}S_w} \frac{\partial S_w}{\partial_x} + K \frac{\lambda_w \lambda_o}{\lambda_t} (\rho_o - \rho_w) g_x, \quad \ldots (2)$$

where λ_α, $\alpha = o, w$ is the mobility of phase α, defined as $\lambda_\alpha = k_{r\alpha}/\mu_\alpha$; $\lambda_t = \lambda_w + \lambda_o$ is the total mobility; $q_t = q_o + q_w$ is the total velocity of water and oil; K is the absolute permeability; p_c is the capillary pressure defined as the difference between the oil and water pressure, or $p_c = p_o - p_w$; ρ_α is the density of phase α; and g_x is the gravitational acceleration in the flow direction. The equation for q_w shows that water velocity is a result of the total velocity, a gradient in capillary pressure and gravity, as represented by the first, second, and third terms of the right-hand side of Eq. 2, respectively.

Analytical Solutions for Capillary-Dominated Cases

If we ignore capillary forces (the second term in Eq. 2 is set to zero), the Buckley-Leverett solution can be constructed. We will not repeat the analysis here because it is standard in the literature (Buckley and Leverett 1942; Dake 1983). The key point for our analysis is that, for a smooth varation in saturation (that is, ignoring the shock), we can write

$$x(S_w, t) = \frac{q_t}{\phi} f_w'(S_w) t, \quad \ldots\ldots\ldots\ldots\ldots\ldots\ldots\ldots (3)$$

for a fixed injection rate q_t. The total flow rate q_t is a free parameter; it is imposed as a boundary condition and its value scales the speed with which the water moves. If we ignore gravitational forces, the fractional flow of the water phase is defined as $f_w = \lambda_w/\lambda_t$.

The Buckley-Leverett Analog for Capillary-Dominated Flow. We now consider solutions to Eq. 1, including capillary pressure but ignoring gravitational forces (the third term in Eq. 2). In both cases, there is no forced injection of water (the wetting phase), but water spontaneously enters the porous medium under the action of capillary forces only. We also neglect nonequilibrium effects, which have been observed in the literature (Barenblatt et al. 1990; Le Guen and Kovscek 2006) because the model encapsulated in Eqs. 1 and 2 allows us to match our experimental data, as will be shown later.

The case we consider first is cocurrent flow, where the imbibing phase (water) enters the inlet and the displaced phase (oil) escapes from the opposite end. Oil and water flow in the same direction. In this case, there is a finite total velocity. The water velocity, from Eq. 2, is

$$q_w = f_w(S_w) q_t + K \frac{\lambda_w \lambda_o}{\lambda_t} \frac{\mathrm{d}p_c}{\mathrm{d}S_w} \frac{\partial S_w}{\partial_x}. \quad \ldots\ldots\ldots\ldots\ldots\ldots (4)$$

For the countercurrent case, water invades a closed system, and therefore oil leaves in the opposite direction to the water. In this case $q_o = -q_w$, which yields $q_t = 0$ and leads to

$$q_w = K \frac{\lambda_w \lambda_o}{\lambda_t} \frac{\mathrm{d}p_c}{\mathrm{d}S_w} \frac{\partial S_w}{\partial x}. \quad \ldots\ldots\ldots\ldots\ldots\ldots\ldots (5)$$

Notice the extra term for q_w in the cocurrent case. This implies that even if all petrophysical properties are the same, q_w in the cocurrent and countercurrent cases will be different. Because $f_w(S_w)q_t$ is positive, q_w will be larger than the inflow for the countercurrent case. This is indeed observed in experiments and numerical tests (Bourbiaux and Kalaydjian 1990; Pooladi-Darvish and Firoozabadi 2000; Chen et al. 2003) that show that production rates from cocurrent imbibition are always larger than those from countercurrent SI on the same rock. $f_w(S_w)q_t$ is known as the "viscous-coupling" term. Obviously, if f_w is small compared with the capillary term over the saturation range that is relevant for SI, then the viscous-coupling term will be small, and the difference between cocurrent and countercurrent SI becomes negligible. This is the case for mixed-wet systems or where the displaced phase has a low viscosity, such as air, which we will discuss further.

Let us return to finding an analytical solution for SI. From Eqs. 1 and 2, the conservation equation for S_w can be reduced to a nonlinear diffusion equation:

$$\phi \frac{\partial S_w}{\partial t} = \frac{\partial}{\partial x}\left[D(S_w)\frac{\partial S_w}{\partial x}\right] \text{(countercurrent case)}$$

and

$$\phi \frac{\partial S_w}{\partial t} = q t f_w' \frac{\partial S_w}{\partial x} + \frac{\partial}{\partial x}\left[D(S_w)\frac{\partial S_w}{\partial x}\right] \text{(cocurrent case)}. \quad \ldots\ldots\ldots\ldots\ldots\ldots (6)$$

We have introduced the nonlinear capillary-diffusion coefficient, with units of length squared over time (Barenblatt et al. 1990):

$$D(S_w) = -K \frac{\lambda_w \lambda_o}{\lambda_t} \frac{\mathrm{d}p_c}{\mathrm{d}S_w}. \quad \ldots\ldots\ldots\ldots\ldots\ldots\ldots (7)$$

Note that $D(S_w)$ is zero if $S_w = S_{wir}$. The implication of this, as we show later, is that the saturation gradient will diverge at the leading edge of the imbibition front, where $S_w = S_{wir}$. We will find an analytical solution for Eq. 6 together with the boundary and initial conditions:

$$S_w(x = 0, t) = S_{w,\max}$$
$$S_w(x > 0, t = 0) = S_{wir}. \quad \ldots\ldots\ldots\ldots\ldots\ldots\ldots (8)$$

The injection condition is the maximum water saturation $S_{w,\max}$ possible under SI, and is the value where the capillary pressure is zero, or $p_c(S_{w,\max}) = 0$. For weakly water-wet and mixed-wet media, $S_{w,\max}$ may be less than the maximum water saturation achievable for forced displacement, where the capillary pressure may be negative. The initial condition is a uniform water saturation, which we assume is the residual or connate value; that is, the water has zero relative permeability. The approach we follow is derived from the theory of nonlinear dispersive partial-differential equations (Tao 2006). The formal derivation has been developed previously (McWhorter and Sunada 1990; Schmid et al. 2011).

We motivate the solution by considering measurements of saturation profiles for SI in Ketton limestone shown in **Fig. 1.** Similar profiles have been measured by Le Guen and Kovscek (2006) and Zhou et al. (2002). **Fig. 2** shows the average saturation as a function of distance from the inlet divided by the square root of the time since the start of the displacement for the experiment shown in Fig. 1 and for an experiment in diatomite (Zhou et al. 2002). **Fig. 3** shows the capillary pressure and relative permeabilities used in the analytical solution, which we discuss later. To a good approximation, the measurements fall onto one curve for different times. Whenever two different times and locations satisfy $x_1/\sqrt{t_1} = x_2/\sqrt{t_2}$, then also the saturation values at x_1 and x_2 are the same at the respective times t_1 and t_2. Although the distance traveled by any saturation level is proportional to $\sqrt{t}$, different saturation levels are transported with different overall velocity, and not simultaneously. Therefore, the distance traveled must also be a function of saturation. This is similar to the Buckley-Leverett theory, but the key difference is that the diffusive nature of Eq. 6 gives rise to a $\sqrt{t}$ dependence rather than a linear dependence in time. Why do we see this diffusive behavior? If we have a displacement controlled entirely by capillary forces, then the driving force is simply the capillary pressure, which remains fixed for a given saturation. However, from Darcy's law, the flow rate is proportional to the pressure gradient. Hence, if the saturation has moved a distance x, then the pressure gradient is proportional to $1/x$. The flow rate gives the speed of movement $\mathrm{d}x/\mathrm{d}t$ and hence a simple integration gives $x^2 \approx t$ or $x \approx \sqrt{t}$.

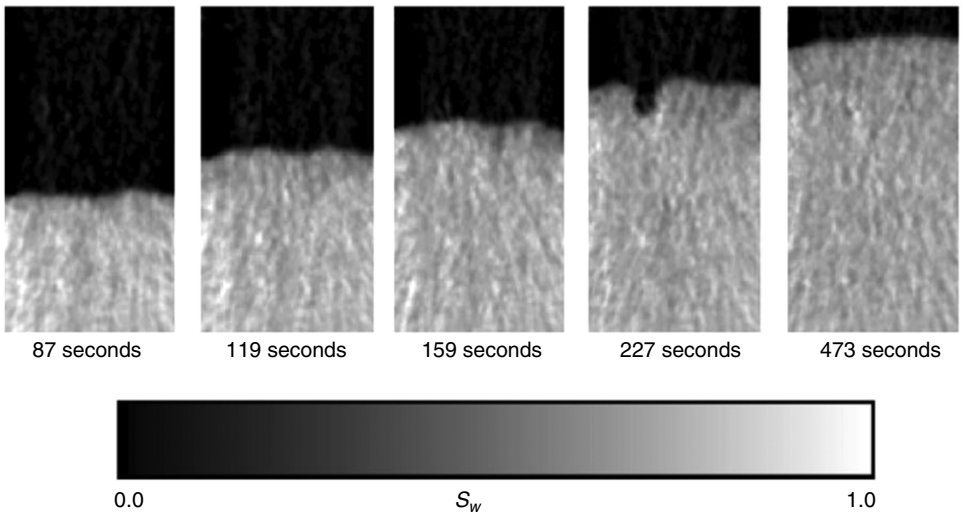

Fig. 1—Measured SI profiles for a cocurrent experiment. The saturation front moves into the core with a time dependence of $\sqrt{t}$. This observation can be used for constructing an analytical solution. In the experiment, water imbibes from the base of a Ketton-limestone-core sample, whereas air (the displaced phase in this case, as opposed to oil) escapes from the top. The saturation profiles are measured by use of X-ray computed tomography scanning.

By use of this physical observation, we introduce the similarity variable $\omega = x/\sqrt{t}$ and attempt to find solutions for S_w that are a function of ω only (Barenblatt et al. 1990):

$$\omega = \frac{x}{\sqrt{t}},\ S_w = S_w(\omega). \quad \ldots\ldots\ldots\ldots\ldots\ldots\ldots\ldots\ (9)$$

Because the distance traveled by a given saturation value is proportional to $\sqrt{t}$, the water volume imbibed must be proportional to $\sqrt{t}$. Therefore, q_w ($x = 0$, t) scales as $1/\sqrt{t}$. This means that we can find a proportionality constant C in m/$\sqrt{\text{s}}$ units (C^2 has the units of a diffusion coefficient, as does D in Eq. 7), for which we can write

$$q_w(x=0,t) = \frac{C}{\sqrt{t}},$$
$$Q_w(t) = \int_{t=0}^{t} q_w(x=0,t)\,dt = 2C\sqrt{t}. \quad \ldots\ldots\ldots\ldots\ (8)$$

The magnitude of C determines how fast the water spontaneously imbibes, and therefore depends on the properties of the rock and fluids, such as the wetting properties, fluid viscosities, and relative and absolute permeabilities. Also, it is clear that because q_w is different for cocurrent and countercurrent flow, C must be different for these two cases as well. Once we know how to calculate C, we have a simple way of quantifying how rock and fluid properties influence a rock's ability to imbibe in cocurrent and countercurrent mode (this is discussed later with our examples).

The key new step to finding a general solution is to write the solution in terms of the derivative of a fractional-flow function F (Schmid et al. 2011):

$$\omega(S_w) = \frac{2C}{\phi}F'(S_w). \quad \ldots\ldots\ldots\ldots\ldots\ldots\ldots\ (11)$$

Eq. 11 is formally identical to the Buckley-Leverett solution, which is Eq. 3. We therefore consider F to be the fractional-flow function for the case of capillary-driven flow, and we hypothesize that F is given by the ratio of the water flow as a function of saturation to its maximum value:

$$F = \frac{q_w}{q_w(S_{w,\max})}. \quad \ldots\ldots\ldots\ldots\ldots\ldots\ldots\ (12)$$

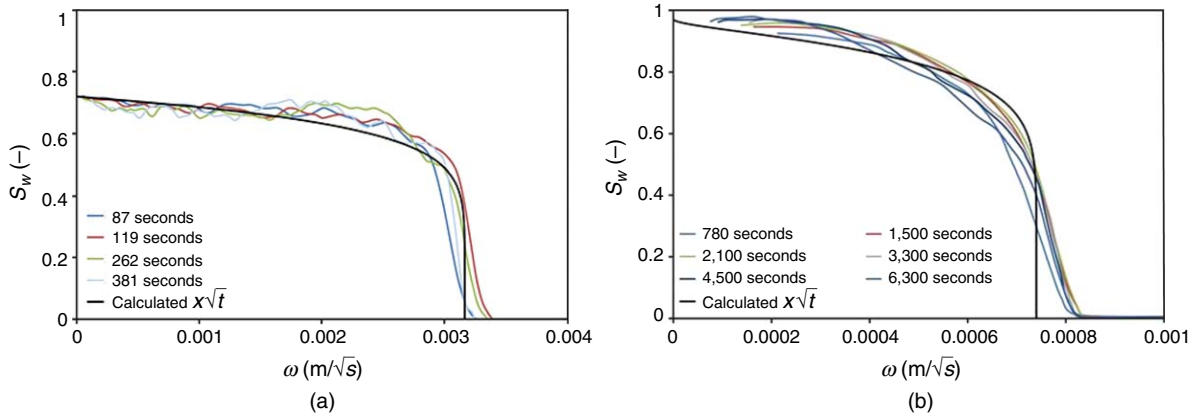

Fig. 2—The saturation profiles from Fig. 1, showing the average saturation along the flow direction for Ketton limestone in (a) cocurrent flow and (b) for diatomite for countercurrent flow obtained from Zhou et al. (2002). The profiles are plotted as functions of $x\sqrt{t}$, where x is the distance moved in the flow direction and t is the time since the beginning of the experiment. To a reasonable approximation, profiles measured at different times fall onto one universal curve. This indicates that the solution for capillary-dominated displacement in one dimension can be written as a function of $x\sqrt{t}$ only. We use this insight to construct analytical solutions. Solutions that match the experiments are shown by the solid black lines. The multiphase-flow properties used for this match are shown in Table 1, while the relative permeabilities and capillary pressure are shown in Fig. 3.

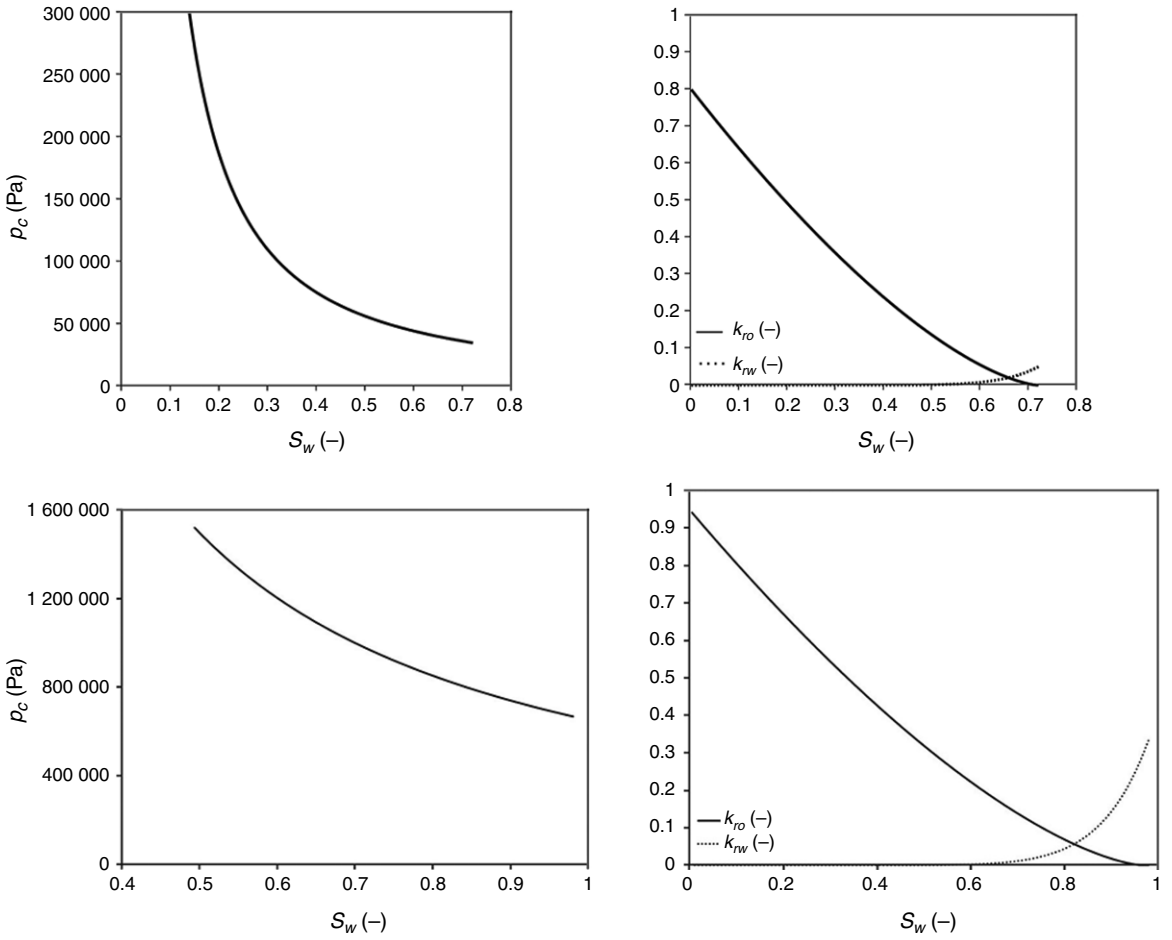

Fig. 3—Relative permeabilities and capillary pressure used to construct the analytical solution shown. As expected, the curves show water-wet characteristics for (top) Ketton limestone and (bottom) diatomite.

There is one important difference between $Q_w(t)$ in the Buckley-Leverett solution and the $Q_w(t)$ we have here. In the Buckley-Leverett theory, $Q_w(t)$ is determined from the imposed injection rate. For the case of capillary-controlled flow, however, C and consequently $Q_w(t)$ cannot be imposed, but are determined by the rock's ability to spontaneously imbibe water; thus, C is a parameter that describes an intrinsic property of the rock/fluid pair. In what follows, we will use the following relation from Eq. 11:

$$\frac{\mathrm{d}\omega}{\mathrm{d}S_w} = \frac{2C}{\phi} F''(S_w). \quad \ldots\ldots\ldots\ldots\ldots\ldots\ldots\ldots \quad (13)$$

We now rewrite the derivatives of the water saturation:

$$\frac{\partial S_w}{\partial t} = \frac{\mathrm{d}S_w}{\mathrm{d}\omega}\frac{\partial \omega}{\partial t} = -\omega \cdot \frac{1}{2t}\frac{\mathrm{d}S_w}{\mathrm{d}\omega},$$
$$\frac{\partial S_w}{\partial x} = \frac{\mathrm{d}S_w}{\mathrm{d}\omega}\frac{\partial \omega}{\partial x} = \frac{1}{\sqrt{t}}\frac{\mathrm{d}S_w}{\mathrm{d}\omega}. \quad \ldots\ldots\ldots\ldots\ldots\ldots\ldots\ldots \quad (14)$$

By use of Eq. 14, the saturation equation, Eq. 6, can be rewritten as an ordinary-differential equation that is much simpler to solve because we only have to deal with total derivatives:

$$\omega\frac{\mathrm{d}S_w}{\mathrm{d}\omega} + 2\frac{\mathrm{d}}{\mathrm{d}\omega}\left[D(S_w)\frac{\mathrm{d}S_w}{\mathrm{d}\omega}\right] = 0 \quad \text{(countercurrent case)}$$
$$\omega\frac{\mathrm{d}S_w}{\mathrm{d}\omega} + 2\frac{\mathrm{d}}{\mathrm{d}\omega}\left[D(S_w)\frac{\mathrm{d}S_w}{\mathrm{d}\,\omega}\right] - 2Cf_w'(S_w)\frac{\mathrm{d}S_w}{\mathrm{d}\omega} = 0 \quad \text{(cocurrent case)}, \quad \ldots\ldots\ldots\ldots\ldots\ldots\ldots\ldots \quad (15)$$

where for the cocurrent case we have used Eq. 10 to substitute for q_t.

Eq. 14 can also be used to check that F truly is the fractional-flow function and satisfies Eq. 12. By inserting $q_w(S_w) = q_w(S_{w,\max})F(S_w)$ from Eq. 5 into the original conservation equation, Eq. 6, we again obtain Eq. 11, which confirms the hypothesis in Eq. 12.

To remove the second-order derivatives, from Eq. 15, we integrate once

$$\int \omega d\, S_w = \frac{2D}{\phi}\frac{\mathrm{d}S_w}{\mathrm{d}\omega} \quad \text{(countercurrent case)},$$
$$\int [\omega - 2Cf_w'(S_w)]\mathrm{d}S_w = -\frac{2D}{\phi}\frac{ES_w}{\mathrm{d}\omega} \quad \text{(cocurrent case)}, \quad \ldots\ldots\ldots\ldots\ldots\ldots\ldots\ldots \quad (16)$$

where the integration constant is zero because $D(S_{wir}) = 0$, and because F is the fractional-flow function $F(S_{wir}) = 0$. We now substitute $\omega \mathrm{d}S_w = 2C/\phi \mathrm{d}F$ and $dS_w/d\omega = \phi/2CF''(S_w)$ from Eq. 13. This leads to a second-order ordinary-differential equation for F:

$$FF'' = -\frac{\phi}{2C^2}D \quad \text{(countercurrent case)},$$
$$(F - f_w)F'' = -\frac{\phi}{2C^2}D \quad \text{(cocurrent case)}. \quad \ldots\ldots\ldots\ldots \quad (17)$$

Eq. 17 is the main mathematical result of this paper. From Eq. 17, we can determine F and C, and once they are known, F' and C can be inserted into Eq. 11 to obtain the saturation profile. To determine F, F', and C from Eq. 17, two possibilities exist. Formally, to obtain a closed-form expression for F and C, Eq. 18 can

be integrated twice. This then leads to F and C being defined implicitly through two integral equations. McWhorter and Sunada (1990), Schmid et al. (2011), and Bjørnara and Mathias (2013) solved these integral equations to obtain solutions; instead, we propose a simple backward-differencing scheme to solve the equations numerically.

The resulting algorithm is simple and can readily be used in a spreadsheet. This solution procedure is described in the next section. Before proceeding, however, we will briefly summarize the two important assumptions in this analysis. We assume incompressible 1D flow in an infinite medium. The solution is valid for a finite system until the leading edge of the saturation reaches the boundary. The time t^* when the solutions stop being valid in a finite matrix block of length L can be obtained from setting $x(S_w,t^*)=L$, which yields

$$t^* = \left[\frac{L\phi}{2CF'(S_{wir})}\right]^2. \quad \ldots\ldots\ldots\ldots\ldots\ldots\ldots\ldots (18)$$

The time until t^* is called "early-time imbibition," up to which our solutions are valid.

The second assumption we make is that the inlet-flow rate declines as $1\sqrt{t}$ (Eq. 10). This can be rigorously proved as the correct boundary condition for SI controlled by capillary forces only (Schmid et al. 2011). However, when gravitational effects become significant, the solutions are no longer accurate, because the flow rate will either be enhanced (for instance, if the denser wetting fluid is moving downward) or suppressed (the denser wetting phase is moving upward).

A Simple Way to Obtain $F(S_w)$ and C Numerically. In this subsection, we describe how to obtain an approximation of arbitrary accuracy for F and C from Eq. 17. We determine F'' from a backward-differencing approximation, and then iteratively determine $F(S_w)$ at a finite number n of saturation points S_{wj}, $j=1,\ldots,n$ that are distributed evenly with a distance ΔS_w between the residual and the maximum water saturation. Because F also depends on the unknown constant C, we also need to iterate on C; therefore, we start with a guessed value of C and continue changing it until $F(S_w)$ converges to the correct solution. We assess convergence by testing if our computed value of $F(S_w=S_{wir})=0$.

The backward-difference scheme yields

$$F''(S_w) \approx \frac{F(S_w+2\Delta S_w)-2F(S_w+\Delta S_w)+F(S_w)}{\Delta S_w^2}. \quad \ldots\ldots\ldots\ldots\ldots\ldots (19)$$

We now replace F'' in Eq. 17 with the approximation and rearrange. For the countercurrent case, this leads to

$$F(S_w) = [F(S_w+\Delta S_w) - 0.5F(S_w+2\Delta S_w)] + \sqrt{[F(S_w+\Delta S_w) - 0.5F(S_w+2\Delta S_w)]^2 - \left(\frac{\phi}{2C^2}\right)D(S_w)\Delta S_w^2}, \quad \ldots\ldots\ldots\ldots\ldots\ldots (20)$$

and for the cocurrent case, we have

$$F(S_w) = [F(S_w+\Delta S_w) - 0.5F(S_w+2\Delta S_w) + 0.5f_w(S_w)] + \sqrt{0.25[F(S_w+2\Delta S_w) - 2F(S_w+\Delta S_w) - f_w(S_w)]^2 - \left\{f_w(S_w)[F(S_w+2\Delta S_w) - 2F(S_w+\Delta S_w)] + \left(\frac{\phi}{2C^2}\right)D(S_w)\Delta S_w^2\right\}}. \quad \ldots\ldots\ldots\ldots\ldots\ldots (21)$$

We therefore can find an approximation of $F(S_w)$ if we know $F(S_w+\Delta S_w)$ and $F(S_w+2\Delta S_w)$ for some starting value $F(S_{w,\text{start}})$. As the two starting values, we take $F(S_{w,\max})=1$ and $F(S_{w,\max}-\Delta S_w)$. The latter can be obtained by recalling that $F'(S_{w,\max})$ can be approximated by a Taylor series:

$$F(S_{w,\max}-\Delta S_w) = \underbrace{F(S_{w,\max})}_{=1} - \underbrace{\Delta S_w F'(S_{w,\max})}_{=0} = 1, \quad \ldots\ldots\ldots\ldots\ldots\ldots (22)$$

where we used the assumption that the maximum saturation is not transported into the medium, and hence $F'(S_{w,\max})=0$.

Eq. 20 requires that we know C. If we knew C exactly, we could approximate $F(S_w)$ at all discrete saturation points. However, C is also unknown and must be determined from Eq. 20 together with F. This can easily be achieved by choosing a starting value for C and then continuing to change it until some convergence criteria for F are met. We can obtain two equivalent convergence criteria by recalling some physical properties of the solution. The first criterion is that we know that $F(S_w)$ is a fractional-flow function, and hence

$$F(S_{wir})=0. \quad \ldots\ldots\ldots\ldots\ldots\ldots\ldots\ldots (23)$$

For the second criterion, we simply use that the fact because of mass balance, the integrated saturation curve must equal the total pore volume imbibed; that is,

$$\int_{S_{wir}}^{S_{w,\max}} x(S_w,t)\,\mathrm{d}S_w = \frac{Q_w(t)}{\phi} = \frac{2C\sqrt{t}}{\phi}. \quad \ldots\ldots\ldots\ldots (24)$$

We approximate the integral and rearrange Eq. 24 by use of Eqs. 9 and 11 to give

$$\sum_{i=1}^{n} F'(S_w,i)\cdot\Delta S_w \approx \frac{Q_w(t)}{\phi} = \frac{\phi}{2C\sqrt{t}} = 1. \quad \ldots\ldots\ldots (25)$$

To determine C, we start with some value C_{start} and continue to change C until Eqs. 23 and 25 are met. The calculation procedure is fairly simple and has been incorporated into a spreadsheet that can be downloaded. The numerical procedure and the use of the spreadsheet are illustrated in the following examples.

Examples: Water-Wet and Mixed-Wet Systems

In the following, three examples are given to illustrate the numerical procedure described previously. They show how to obtain the analytical solution for strongly and weakly water-wet and mixed-wet systems, and also demonstrate how the analytical solutions predict key physical features of water-wet and mixed-wet behavior during SI. The latter is of particular importance because the majority of fractured reservoirs are mixed-wet (Anderson 1987).

The input parameters used in the computations are listed in **Table 1.** In the following, we use power laws for the relative permeability and the capillary pressure curves. Because the analytical solution does not require specific functional forms, other models such as the Brooks-Corey or Van Genuchten (Helmig 1997) could also be used (McWhorter and Sunada 1990; Schmid et al. 2011; Bjørnara and Mathias 2013). The water and oil relative permeabilities are described by

$$k_{rw}(S_w) = k_{rw,\max}\cdot\left(\frac{S_w-S_{wir}}{1-S_{wir}-S_{or}}\right)^{\beta_w},$$
$$k_{ro}(S_o) = k_{ro,\max}\cdot\left(\frac{1-S_w-S_{or}}{1-S_{wir}-S_{or}}\right)^{\beta_w}, \quad \ldots\ldots\ldots (26)$$

where $k_{r\alpha,\max}$, $\alpha=w,o$ is the maximum relative permeability of water or oil, and β_α is the exponent of the relative permeability.

For the capillary pressure curve, we need to distinguish between the water-wet and mixed-wet cases. For the water-wet system, the p_c curve is positive over the whole saturation range, and SI only stops once the water saturation has reached $S_w=1-S_{or}$. The capillary pressure curve is described by

Input Parameters	Strongly Water-Wet Case	Weakly Water-Wet Case	Mixed-Wet Case	Experiment (Ketton)	Experiment (Diatomite)
Initial water saturation	0.2	0.2	0.2	0	0
Residual oil/air saturation	0.4	0.2	0.1	0.28	0.02
Exponent β_w	3	3	3	10	10
$k_{rw,\max}$	0.2	0.5	0.6	0.05	0.3
Exponent β_o	1.5	5	8	1.5	1.5
$k_{ro,\max}$	0.85	0.8	0.8	0.8	0.95
$p_{c,\text{entry}}$ (Pa)	12 000	12 000	12 000	35 000	665 000
Exponent β_{pc}	–0.7	–0.3	–0.2	–1.3	–1.2
Maximum capillary pressure (Pa)	400 000	400 000	400 000	400 000	2 500 000
S_w^*	0.6	0.5	0.32	0.72	0.98
μ_w (Pa·s)	0.001	0.001	0.001	0.001	0.001
μ_o (Pa·s)	0.003	0.001	0.001	10^{-6}	10^{-6}
K (md)	300	300	300	2,381	7
ϕ	0.2	0.2	0.2	0.2	0.7
σ_{ow} (N/m)	0.05	0.05	0.05	0.07	0.07
$C_{\text{cocurrent}}$ ($m/\sqrt{s}$)	9.13×10^{-5}	2.5492×10^{-5}	2.768×10^{-5}	0.0002	–
$C_{\text{countercurrent}}$ ($m/\sqrt{s}$)	4.63×10^{-5}	1.63×10^{-5}	2.733×10^{-5}	–	0.000217

Table 1—Input parameters for calculating the analytical solutions for strongly water-wet, weakly water-wet, and mixed-wet examples and for the cocurrent experiment. For the experiments, the nonwetting phase was air, and the rocks were Ketton carbonate and diatomite.

$$p_c(S_w) = p_{c,\text{entry}} \cdot \left[\frac{(S_w - S_{wir})}{(S_w^* - S_{wir})}\right]^{\beta_{pc}} - p_{c,\text{entry}}, \quad \ldots\ldots\ldots \quad (27)$$

for a capillary entry pressure $p_{c,\text{entry}}$ and an exponent β_{pc}.

For a mixed-wet rock, SI stops at the saturation S^* where p_c becomes zero. In this case, the final recovery is governed by S_w^*, and not by $S_w = 1–S_{or}$. Here, we also use Eq. 27 for p_c, but then Eq. 27 only describes the positive part of the capillary pressure curve that is relevant for SI. The relative permeabilities and capillary pressures we use are shown in **Fig. 4,** while the corresponding capillary-fractional flow F is shown in **Fig. 5.**

Water-Wet Cases. The relative permeabilities and the capillary pressure curve for the water-wet case were chosen such that they show the basic features of a water-wet system. The capillary pressure curve is larger than zero over the whole saturation range; the endpoint value of $k_{rw,\max}$ and k_{rw} itself are small, and the residual saturation S_{or} is relatively large. Because SI can take place over the whole saturation range, the correct boundary value for the water saturation is $S_{w,\max} = 1–S_{or}$.

If C and F are known (Fig. 5), we can determine the S_w profile that is shown in **Fig. 6.** The profile shows the diffusive, smooth behavior typical for SI processes. Notice also that F, contrary to its viscous counterpart f_w, has no inflection point (Fig. 5). Therefore, the saturation profile cannot develop a shock front. In this sense, this makes the SI solution easier to construct than the Buckley-Leverett problem.

From C, we can also determine how fast the rock can imbibe water and expel the oil; **Fig. 7** shows the percentage of total recoverable oil over time from a core of 1-m length. Q_w was calculated from Eq. 10 up to the point when the imbibition front reaches the end of the core at time t^*.

We will now compare the behavior of cocurrent and countercurrent SI. We assume that in both cases we can use the same relative permeabilities, even though the few measurements in the

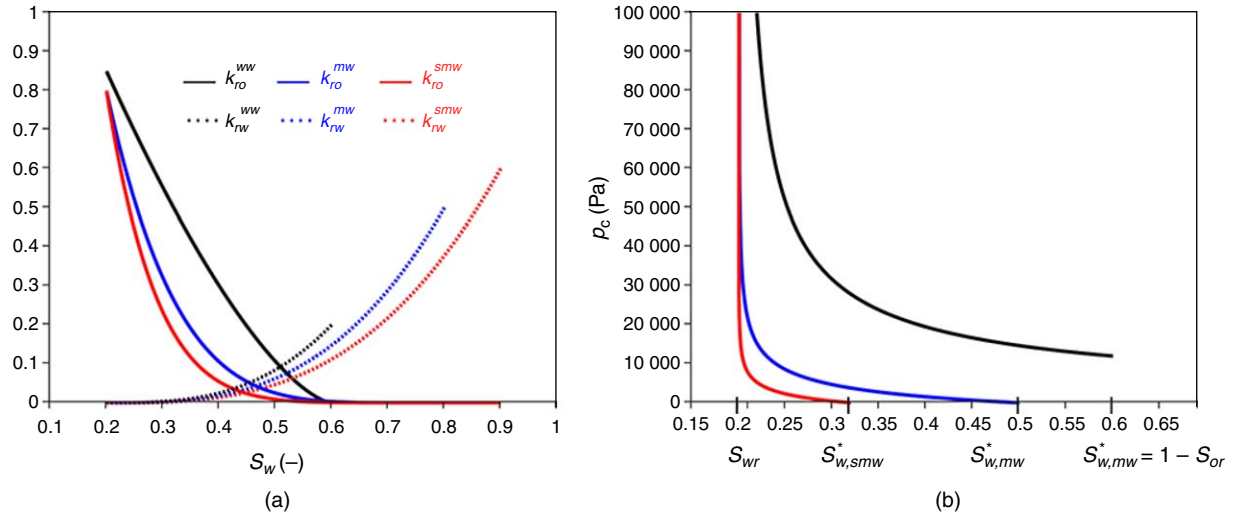

Fig. 4—(a) Relative permeabilities and (b) the positive part of the capillary pressure curve plotted vs. S_w for the strongly water-wet (sww), weakly water-wet (www), and mixed-wet (mw) examples presented in this paper. SI only takes place for positive capillary pressure and stops at S_w^*, which for a mixed-wet system is lower than $1–S_{or}$.

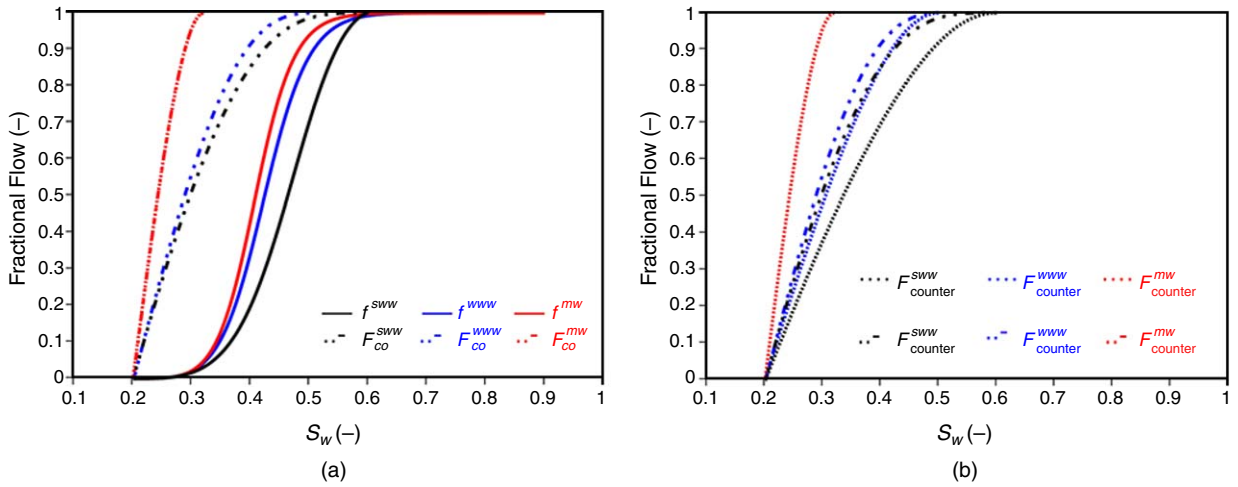

Fig. 5—Fractional-flow functions for (a) spontaneous countercurrent imbibition (dashed and dotted line) and viscous-dominated flow (solid line), and (b) spontaneous countercurrent imbibition (dashed and dotted line) and cocurrent imbibition (dotted line). $F=1$ at $S_w = S_w^*$ because for S_w^*, the capillary pressure p_c becomes zero. Because of the viscous-coupling effect, F for the cocurrent case is always smaller than F for the countercurrent case, leading to higher production rates during cocurrent SI. For mixed-wet systems, however, the viscous-coupling effect becomes negligible. Consequently, the difference between $F^{mw,co}$ and $F^{mw,counter}$ vanishes and the rates of cocurrent and countercurrent SI are similar.

literature indicate that this assumption might not hold (Bourbiaux and Kalaydjian 1990). Once more, we iterate on C until F determined from Eq. 21 has converged. Figs. 5 through 7 show the fractional-flow function, saturation profiles, and production rate, respectively. Compared with the countercurrent case, C is larger and recovery is faster for cocurrent SI. Also, the saturation profile is far less diffused and more piston-like. Both features are characteristic of cocurrent imbibition and are also observed in experiments (Bourbiaux and Kalaydjian 1990; Chen et al. 2003). The reason for this behavior is that for cocurrent SI, q_w additionally depends on $f_w q_t$, which adds to the production rate.

Mixed-Wet Example. We now consider mixed-wet rock. The interplay of relative permeabilites and capillary pressure curves typical of mixed-wet systems determine the size of C and hence production rate (Eq. 10). For mixed-wet systems, SI stops at the saturation S_w^*, where p_c becomes zero. Therefore, the boundary value for the water saturation $S_{w,\max}$ has to be set to this saturation.

The relative permeabilites and capillary pressure curves for the mixed-wet example are chosen such that they represent key features of mixed-wet systems (Behbahani and Blunt 2005; Ryazanov et al. 2009, 2010). The more oil-wetting the system is, the smaller the water saturation at which the capillary pressure goes negative, and the smaller the amount of oil that can be produced by SI.

Fig. 6 shows the comparison of the saturation profiles for the three wettabilities. The cocurrent profiles are again more piston-like than those for countercurrent SI, but as the sample becomes mixed-wet, the difference is small. For the mixed-wet system, the viscous-coupling term becomes negligible because $f_w(S_w)$ is very small in the relevant low-water-saturation range (Fig. 5).

Fig. 7 shows that the percentage of recoverable oil over the recovery rate is much lower for the mixed-wet case because imbibition is impeded by the low water relative permeability at low saturation and relatively low capillary pressure, compared with the water-wet cases. This dramatic increase in imbibition time for mixed-wet rocks has been observed experimentally (Zhou et al. 2000).

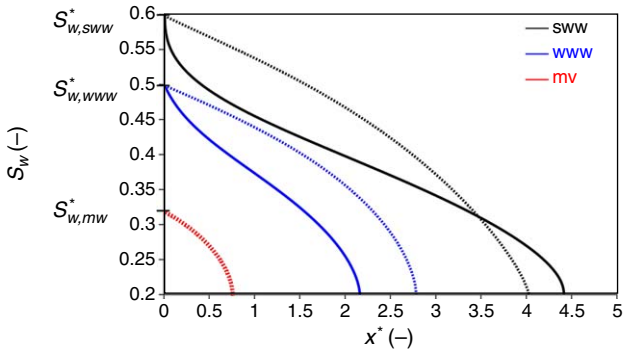

Fig. 6—Normalized saturation profiles for countercurrent SI (solid line) and cocurrent SI (dashed line) as calculated from Eq. 11. The normalized distance $x^*=\phi x/2C\sqrt{t^*}$, where t^* is given by Eq. 18. Cocurrent SI is more piston-like, and thus displacement efficiency is higher for the cocurrent case. For mixed-wet systems, however, the difference between cocurrent and countercurrent SI becomes negligible.

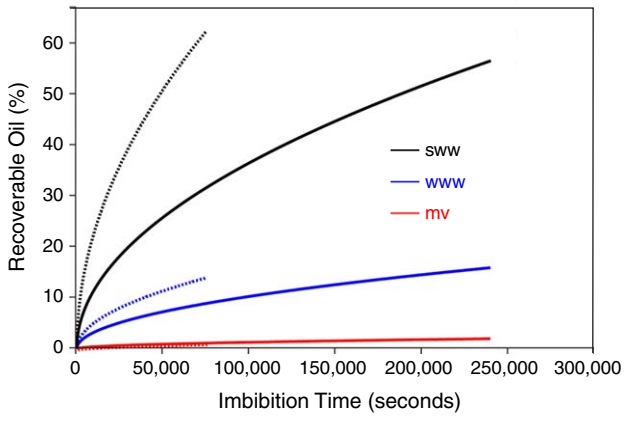

Fig. 7—Percentage of recoverable oil vs. imbibition time up to time t^* (Eq. 18). The fluid and rock properties are given in Table 1, and the length of the core is 1 m. Recovery by cocurrent SI (dashed lines) is faster than that by countercurrent SI (solid lines), and in the water-wet cases strongly so. In the mixed-wet case, the analytical solution predicts much slower recovery. This is because of the combined effect of very-low water relative permeability and low capillary pressure (Fig. 5).

Application: Matching to Experimental Data and a Scaling Group for Field-Scale Simulation

Analysis of Experiments. Fig. 2 shows experimental imbibition profiles scaled as a function of $x\sqrt{t}$. We can match the measurements to an analytical solution by use of the approach shown in this paper through adjusting the relative permeabilities and capillary pressure. The imbibition profile depends on three functions: two relative permeabilities and the capillary pressure. Hence, we cannot determine all three from this experiment alone. If we had measured relative permeabilities (by use of the classical Buckley-Leverett analysis), then the capillary pressure can be determined. In contrast, we could find the water relative permeability if the capillary pressure and oil relative permeability (from a centrifuge experiment, as an example) were known. Overall, the SI profile is a useful complement to other core measurements and can be used to determine multiphase-flow properties.

With an imbibition-saturation profile measured as a function of ω (Eq. 11), we can integrate it to find F and differentiate it to find F'' within the constant C (Eq. 13). C itself is found from the amount of water imbibed (Eq. 10). Then, from Eq. 7, we can determine the capillary dispersion $D(S_w)$ directly. This is a more rigorous and direct approach than that presented by authors such as Zhou et al. (2002), who determined relative permeabilities and capillary pressure from imbibition measurements (such as those shown in Fig. 3) by use of a numerical approach. That is more cumbersome, is prone to numerical error, and did not achieve an exact match.

We adjusted the parameters shown in Table 1 to find a match to the experimental profiles for the SI experiments shown in Fig. 2. The value of C in this case is not obtained iteratively, as in the examples discussed previously, but is also determined experimentally from the relation between $Q_w(t)$ and C (Eq. 10), fitting C to the measured water volume imbibed over time.

The agreement between the calculated S_w profile and the measured one demonstrates that the theoretical predictions do indeed yield saturation profiles similar to those measured experimentally. The slight discrepancies between the experiment and the analytical solutions are likely because of heterogeneity in the rock samples, leading to a nonuniform imbibition profile.

Fig. 3 shows the relative permeabilities and capillary pressure used to construct the analytical solution. In the experiments with water imbibed into dry rock, we expect the system to be strongly water-wet. This is indeed what is observed with a low water relative permeability with a residual air saturation of 0.28 for Ketton limestone. The diatomite used by Zhou et al. (2002) showed weaker water-wet behavior compared with Ketton, with a higher water relative permeability and a low residual saturation.

Scaling Group for Field-Scale Simulation. The second application of this work is to determine scaling groups for use in larger-scale simulation, such as in dual-porosity modeling of fractured reservoirs. Schmid and Geiger (2012) introduced the nondimensional time for SI as the total volume imbibed divided by pore volume:

$$t_d = \left[\frac{Q_w(t)}{\phi L}\right]^2 = \left(\frac{2C}{\phi L}\right)^2. \quad \ldots\ldots\ldots\ldots\ldots\ldots \quad (28)$$

Note that for SI the expression in the brackets needs to be squared because, as we have seen previously, $Q_w(t)$ is proportional to $\sqrt{t}$. Schmid and Geiger (2012; 2013) have shown that this scaling group can be used to reduce experimental measurements of overall recovery as a function of time onto one universal curve, allowing the average SI behavior to be captured elegantly and accurately.

The value of C can be obtained from known relative permeabilities, capillary pressure, and permeability; by use of the approach of this paper; or—as in the experimental example discussed previously—by matching to an analytic solution obtained by adjusting the multiphase-flow properties to provide a good match.

This scaling group can then be used in dual-porosity models of field-scale flow in fractured reservoirs, work that is under development (Di Donato et al. 2007; Geiger et al. 2013; Maier and Geiger 2013; Maier et al. 2013).

Summary and Conclusions

In this paper, the general analytical solutions for SI were derived following McWhorter and Sunada (1990) and Schmid et al. (2011). These solutions allow for important insights into the physics of SI. These insights enable the following:

1. The construction of solutions by use of a simple iterative approach on a spreadsheet.
2. The quantification of wettability effects on imbibition rate, which exhibits a considerable slowing of recovery in mixed-wet systems because of the combined effects of low water relative permeability and capillary pressure.
3. The prediction of significant differences between cocurrent and countercurrent SI, in line with experimental results. Cocurrent imbibition is more piston-like and leads to higher production rates than countercurrent SI. However, for mixed-wet systems, this effect becomes weak and the difference between cocurrent and countercurrent SI becomes negligible.
4. The demonstration of how experimental measurements of saturation profiles in imbibition can be used to obtain or constrain relative permeabilities and capillary pressures by matching experimental measurements to the analytical solutions.

Nomenclature

C = constant that quantifies the rate of SI, m/$\sqrt{\text{s}}$
D = capillary dispersion, m^2
f = fractional flow for viscous-controlled flow
F = fractional flow for capillary-controlled flow
k_r = relative permeability
K = absolute permeability, m^2
L = length of the core, m
p_c = capillary pressure, Pa
P = fluid pressure, Pa
Q_w = cumulative volume imbibed/injected, m
R = recovery, m^3
R_∞ = ultimate recovery, m^3
S = saturation
t = time, seconds
t_d = dimensionless time
β = exponent for the relative permeabilities and capillary pressure
λ = mobility, 1/(Pa·s)
μ = fluid viscosity, Pa/s
σ = interfacial tension, N/m
ϕ = porosity

Acknowledgments

Author K. S. Schmid gratefully acknowledges funding from the German research foundation, DFG, within the International Research Training Group NUPUS. Author S. Geiger is generously supported by the Foundation CMG. Authors M. J. Blunt and N. Alyafei are grateful for support from the Qatar Carbonates and Carbon Storage Research Centre, funded jointly by Qatar Petroleum, Shell, and the Qatar Science and Technology Park.

References

Anderson, W. G. 1987. Wettability Literature Survey Part 5: The Effects of Wettability on Relative Permeability. *J Pet Technol* **39** (11): 1453–1468. SPE-16323-PA. http://dx.doi.org/10.2118/16323-PA.

Barenblatt, G. I., Entov, V. M., and Ryzhik, V. M. 1990. *Theory of Fluid Flows Through Natural Rocks*. Dordrecht, The Netherlands: Springer.

Behbahani, H. and Blunt, M. J. 2005. Analysis of Imbibition in Mixed-Wet Rocks Using Pore-Scale Modeling. *SPE J.* **10** (4): 466–474. SPE-90132-PA. http://dx.doi.org/10.2118/90132-PA.

Bjørnara, T. I. and Mathias, S. A. 2013. A Pseudospectral Approach to the McWhorter and Sunada Equation for Two-Phase Flow in Porous Media with Capillary Pressure. *Computat. Geosci.* **17** (6): 889–897. http://dx.doi.org/10.1007/s10596-013-9360-4.

Bourbiaux, B. and Kalaydjian, F. 1990. Experimental Study of Cocurrent and Countercurrent Flows in Natural Porous Media. *SPE Res Eng* **5** (3): 361–368. SPE-18283-PA. http://dx.doi.org/10.2118/18283-PA.

Buckley, S. E. and Leverett, M. C. 1942. Mechanism of Fluid Displacement in Sands. In *Transactions of the Society of Petroleum Engineers*, Vol. 146, Part 1, SPE-942107-G, 107–116. http://dx.doi.org/10.2118/942107-G.

Chen, Q., Gingras, M. K., and Balcom, B. J. 2003. A Magnetic Resonance Study of Pore Filling Processes During Spontaneous Imbibition in Berea Sandstone. *J. Chem. Phys.* **119:** 9609. http://dx.doi.org/10.1063/1.1615757.

Cil, M. and Reis, J. C. 1996. A Multi-Dimensional, Analytical Model for Countercurrent Water Imbibition into Gas-Saturated Matrix Blocks. *J. Pet. Sci. Eng.* **16** (1–3): 61–69. http://dx.doi.org/10.1016/0920-4105(95)00055-0.

Dake, L. P. 1983. *Fundamentals of Reservoir Engineering*, Vol. 8. Amsterdam: Elsevier Science.

Di Donato, G., Lu, H., Tavassoli, Z. et al. 2007. Multirate-Transfer Dual-Porosity Modeling of Gravity Drainage and Imbibition. *SPE J.* **12** (1): 77–88. SPE-93144-PA. http://dx.doi.org/10.2118/93144-PA.

Geiger, S., Dentz, M., and Neuweiler, I. 2013. A Novel Multi-Rate Dual-Porosity Model for Improved Simulation of Fractured and Multiporosity Reservoirs. *SPE J.* **18** (4): 670–684. SPE-148130-PA. http://dx.doi.org/10.2118/148130-PA.

Helmig, R. 1997. *Multiphase Flow and Transport Processes in the Subsurface*. Berlin: Springer.

Kashchiev, D. and Firoozabadi, A. 2002. Analytical Solutions for 1D Countercurrent Imbibition in Water-Wet Media. *SPE J.* **8** (4): 401–408. SPE-87333-PA. http://dx.doi.org/10.2118/87333-PA.

Le Guen, S. S. and Kovscek, A. R. 2006. Nonequilibrium Effects During Spontaneous Imbibition. *Transport Porous Med.* **63** (1): 127–146. http://dx.doi.org/10.1007/s11242-005-3327-4.

Maier, C. and Geiger, S. 2013. Combining Unstructured Grids, Discrete Fracture Representation and Dual-Porosity Models for Improved Simulation of Naturally Fractured Reservoirs. Presented at the SPE Reservoir Characterization and Simulation Conference and Exhibition, Abu Dhabi, 16–18 September. SPE-166049-MS. http://dx.doi.org/10.2118/166049-MS.

Maier, C., Schmid, K. S., Elfeel, M. A. et al. 2013. Multi-Rate Mass-Transfer Dual-Porosity Modelling Using the Exact Analytical Solution for Spontaneous Imbibition. Presented at the EAGE Annual Conference and Exhibition Incorporating SPE Europec, London, 10–13 June. SPE-164926-MS. http://dx.doi.org/10.2118/164926-MS.

Mason, G. and Morrow, N. R. 2013. Developments in Spontaneous Imbibition and Possibilities for Future Work. *J. Pet. Sci. Eng.* **110** (October): 268–293. http://dx.doi.org/10.1016/j.petrol.2013.08.018.

McWhorter, D. B. and Sunada, D. K. 1990. Exact Integral Solutions for Two-Phase Flow. *Water Resour. Res.* **26** (3): 399–413. http://dx.doi.org/10.1029/WR026i003p00399.

McWhorter, D. B. and Sunada, D. K. 1992. Exact Integral Solutions for Two-Phase Flow: Reply. *Water Resour. Res.* **28** (5): 1479. http://dx.doi.org/10.1029/92WR00474.

Pooladi-Darvish, M. and Firoozabadi, A. 2000. Cocurrent and Countercurrent Imbibition in a Water-Wet Matrix Block. *SPE J.* **5** (1): 3–11. SPE-38443-PA. http://dx.doi.org/10.2118/38443-PA.

Ryazanov, A. V., van Dijke, M. I. J., and Sorbie, K. S. 2009. Two-Phase Pore-Network Modelling: Existence of Oil Layers During Water Invasion. *Transport Porous Med.* **80** (1): 79–99. http://dx.doi.org/10.1007/s11242-009-9345-x.

Ryazanov, A. V., van Dijke, M. I. J., and Sorbie, K. S. S. 2010. Pore-Network Prediction of Residual Oil Saturation Based on Oil Layer Drainage in Mixed-wet Systems. Presented at the SPE Improved Oil Recovery Symposium, Tulsa, 24–28 April. SPE-129919-MS. http://dx.doi.org/10.2118/129919-MS.

Schmid, K. S. and Geiger, S. 2012. Universal Scaling of Spontaneous Imbibition for Water-Wet Systems. *Water Resour. Res.* **48** (3): W03507. http://dx.doi.org/10.1029/2011WR011566.

Schmid, K. S. and Geiger, S. 2013. Universal Scaling of Spontaneous Imbibition for Arbitrary Petrophysical Properties: Water-Wet and Mixed-Wet States and Handy's Conjecture. *J. Pet. Sci. Eng.* **101** (January): 44–61. http://dx.doi.org/10.1016/j.petrol.2012.11.015.

Schmid, K. S., Geiger, S., and Sorbie, K. S. 2011. Semianalytical Solutions for Co- and Countercurrent Imbibition and Dispersion of Solutes in Immiscible Two-Phase Flow. *Water Resour. Res.* **47** (2): W02550. http://dx.doi.org/10.1029/2010WR009686.

Tao, T. 2006. *Nonlinear Dispersive Equations: Local and Global Analysis*. Providence, Rhode Island: American Mathematical Society.

Yortsos, Y. C. and Fokas, A. S. 1983. An Analytical Solution for Linear Waterflood Including the Effects of Capillary Pressure. *SPE J.* **23** (1): 115–124. SPE-9407-PA. http://dx.doi.org/10.2118/9407-PA.

Zhou, D., Jia, L., Kamath, J. et al. 2002. Scaling of Counter-Current Imbibition Processes in Low-Permeability Porous Media. *J. Pet. Sci. Eng.* **33** (1–3): 61–74. http://dx.doi.org/10.1016/S0920-4105(01)00176-0.

Zhou, X., Morrow, N. R., and Ma, S. 2000. Interrelationship of Wettability, Initial Water Saturation, Aging Time, and Oil Recovery by Spontaneous Imbibition and Waterflooding. *SPE J.* **5** (2): 199–207. SPE-62507-PA. http://dx.doi.org/10.2118/62507-PA.

Karen S. Schmid is a consultant at The Boston Consulting Group, the world's leading strategic management consulting firm. Previously, she held a post-doctoral-degree position at the Department of Hydromechanics and Modeling of Hydrosystems at the University of Stuttgart, Germany. Schmid is a member of SPE. She holds a PhD degree from the Institute of Petroleum Engineering at Heriot-Watt University in Edinburgh, and a master's degree in applied mathematics from the Technical University of Munich.

Nayef M. Alyafei is an assistant professor at Texas A&M University at Qatar. He has been with Texas A&M University at Qatar since 2015. Alyafei's current research interests include wettability and SI studies as well as pore-scale imaging and modeling. He has authored or coauthored nine technical papers. Alyafei is a member of SPE. He holds a PhD degree in petroleum engineering from Imperial College London.

Sebastian Geiger is the Foundation CMG Chair in Carbonate Reservoir Simulation at the Institute of Petroleum Engineering at Heriot-Watt University. He joined Heriot-Watt University as a lecturer (assistant professor) in 2006 and was promoted to senior lecturer (associate professor) in 2009 and to full professor in 2010. Geiger has authored more than 110 technical papers in the areas of modeling and simulating flow in (fractured) carbonate formations. He serves on several technical committees for SPE and was the cochair of the joint American Association of Petroleum Geologists/SPE/Society of Exploration Geophysicists Hedberg Research Conference on Fundamental Controls on Flow in Carbonates. Geiger holds a PhD degree from ETH Zurich and a master's degree from Oregon State University.

Martin J. Blunt is the Shell Professor of Petroleum Engineering at Imperial College London. Previously, he was an associate professor of petroleum engineering at Stanford University and worked at the BP Research Centre. Blunt is a Distinguished Member of SPE, was awarded the 1996 SPE Cedric K. Ferguson Medal and the 2011 SPE Lester C. Uren Award, served as associate executive editor for *SPE Journal* from 1996 to 1998, and was a member of the *SPE Journal* Editorial Board from 1996 to 2005. He was also a 2001 SPE Distinguished Lecturer. Blunt holds master's and PhD degrees in physics from Cambridge University.